

General Disclaimer

One or more of the Following Statements may affect this Document

- This document has been reproduced from the best copy furnished by the organizational source. It is being released in the interest of making available as much information as possible.
- This document may contain data, which exceeds the sheet parameters. It was furnished in this condition by the organizational source and is the best copy available.
- This document may contain tone-on-tone or color graphs, charts and/or pictures, which have been reproduced in black and white.
- This document is paginated as submitted by the original source.
- Portions of this document are not fully legible due to the historical nature of some of the material. However, it is the best reproduction available from the original submission.

(NASA-CR-152302) DEVELOPMENT OF CRYOGENIC
THERMAL CONTROL HEAT PIPES Final Report (B
& K Engineering, Inc., Towson, Md.) 40 p
HC A03/MF A01 CSCL 20D

N79-30499

G3/34 Unclass
15385

BK042-1012

FINAL REPORT
FOR
DEVELOPMENT OF CRYOGENIC
THERMAL CONTROL HEAT PIPES

August 1978

Prepared for
NASA Ames Research Center
Under
Contract No. NAS2-9613

By
H. J. Suelau
B & K ENGINEERING, INC.
Suite 825, One Investment Place
Towson, Maryland 21204

CONTENTS

	<u>Page</u>
ILLUSTRATIONS	iii
TABLES	iv
1.0 INTRODUCTION	1
2.0 DETAILED DESIGN	2
2.1 Axially Grooved Stainless Steel Tubing	2
2.2 Liquid Trap Diode Heat Pipe	5
2.3 Thermal Switch Heat Pipe	7
2.4 Hybrid Variable Conductance Heat Pipe	9
3.0 FABRICATION AND PROCESSING	11
3.1 General	11
3.2 Integrity Verification	11
4.0 THERMAL TESTING	13
4.1 General	13
4.2 Liquid Trap Diode Heat Pipe	13
4.3 Thermal Switch Heat Pipe	20
4.4 Hybrid VCHP	23
5.0 CONCLUSIONS AND RECOMMENDATIONS	32
6.0 REFERENCES	36

ILLUSTRATIONS

<u>Figure No.</u>		<u>Page</u>
2-1	Enlarged cross-section of stainless steel axially grooved tubing	3
4-1	HEPP liquid trap diode heat pipe instrumentation schematic	14
4-2	Start-up behavior of liquid trap diode heat pipe under a 2-W load	15
4-3	Forward mode heat transport capability of liquid trap diode	17
4-4	Reversal and recovery behavior of the liquid trap diode heat pipe	19
4-5	Thermal switch heat pipe instrumentation schematic	21
4-6	Heat transport capability vs. elevation for thermal switch heat pipe	22
4-7	Axial profiles of thermal switch heat pipe during switching operation	24
4-8	Hybrid VCHP instrumentation schematic	25
4-9	Start-up behavior of VCHP/hybrid	26
4-10	Heat transport capability vs. elevation for Hybrid VCHP	28
4-11	Hybrid VCHP diode reversal behavior	32

TABLES

<u>Table No.</u>		<u>Page</u>
2-1	Geometric characteristics of axially grooved tubing for liquid trap diode heat pipe	4
2-2	Liquid trap diode heat pipe design summary . . .	6
2-3	Thermal switch heat pipe design summary	8
2-4	Variable conductance heat pipe design summary . .	10
3-1	Pressure retention characteristics of TCHP's . .	12
4-1	HEPP liquid trap diode performance	16
4-2	Summary of Hybrid VCHP gas control tests	30

1.0 INTRODUCTION

The objective of this program was to develop thermal control heat pipes that are applicable to the low temperature to cryogenic range. A previous effort demonstrated that stainless steel axially grooved tubing which met performance requirements could be fabricated.¹ Stainless steel tubing provides a high strength envelope and its low axial conductance is advantageous in variable conductance and diode heat pipe designs. The axially grooved wick structure is desirable because it provides a level of performance which can normally be achieved only by more complex and less reliable composite wick designs.

Three heat pipe designs utilizing stainless steel axially grooved tubing were fabricated and tested in this effort. One is a liquid trap diode heat pipe which conforms to the configuration and performance requirements of the Heat Pipe Experiment Package (HEPP). The HEPP is scheduled for flight aboard the Long Duration Flight Exposure Facility (LDEF). Another is a thermal switch heat pipe which is designed to permit energy transfer at the cooler of the two identical legs. The third thermal component is a hybrid variable conductance heat pipe (VCHP). The design incorporates both a conventional VCHP system and a liquid trap diode.

This report reviews the design, fabrication and thermal testing of these heat pipes. It discusses the demonstrated heat pipe behavior including start-up, forward mode transport, recovery after evaporator "dry-out," diode performance and variable conductance control.

2.0 DETAILED DESIGN

2.1 Axially Grooved Stainless Steel Tubing

The axially grooved wick design was chosen because of its inherently reliable performance. The composite wick designs which provide comparable heat transport are more complex to fabricate and have not demonstrated consistent performance characteristics.

Stainless steel is the preferred material for cryogenic thermal control applications because its high strength permits the use of a thin walled envelope, which, in combination with its already low thermal conductivity, minimizes axial conduction effects. This is especially advantageous in diode applications. Prior to this program, axially grooved heat pipes had not been fabricated with stainless steel because its high strength and low ductility make it difficult to form.¹ A cold forge swaging process was employed to obtain the initial groove form. Multiple drawing and annealing steps were used to bring the tubing to its final divergent groove configuration. The wall thickness was then reduced by centerless grinding.

An enlarged cross-section of the tubing used to fabricate the liquid trap diode is shown in Fig. 2-1. A summary of the geometric characteristics are presented in Table 2-1. The axial conduction of this tubing is less than $0.05 \frac{\text{W-cm}}{^\circ\text{C}}$.

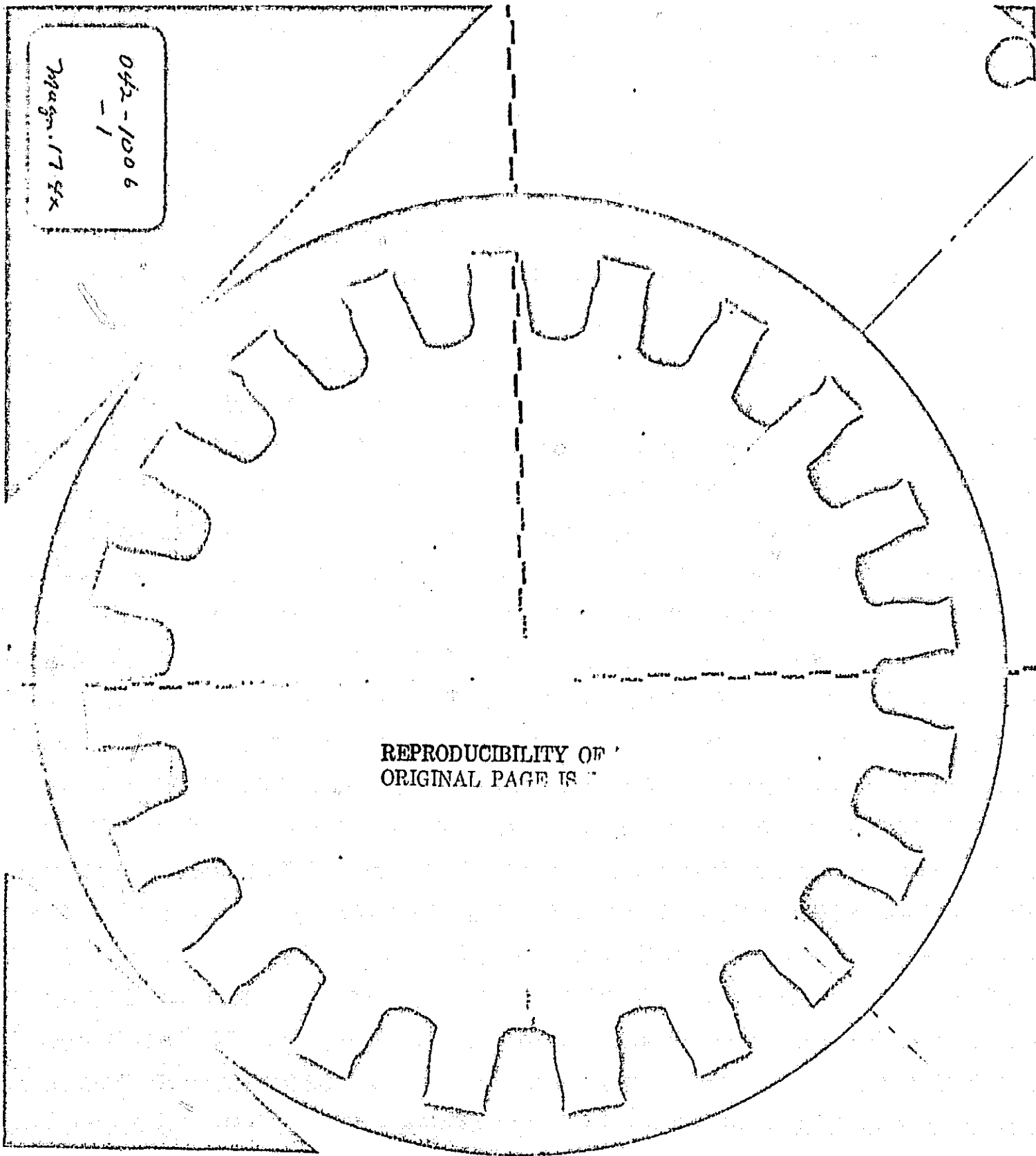


Fig. 2-1. Enlarged cross-section of stainless steel axially grooved tubing

TABLE 2-1

GEOMETRIC CHARACTERISTICS OF AXIALLY GROOVED TUBING FOR
LIQUID TRAP DIODE HEAT PIPE

	<u>mm</u>	<u>in</u>
Number of grooves	20	
Groove width	0.64	0.025
Groove depth	0.95	0.037
Groove aspect ratio	1.48	
Land tip radius	0.18	0.007
Outside diameter	10.50	0.413
Vapor core diameter	7.65	0.301
Wall thickness	0.54	0.021

2.2 Liquid Trap Diode Heat Pipe (LTD)

The liquid trap diode heat pipe is compatible with the configuration requirements of the Heat Pipe Experiment Package (HEPP). The pipe is bent in a U-shape with a 33.3 cm (13-1/8 in.) centerline to centerline separation. A design summary of the heat pipe is presented in Table 2-2 (also see instrumentation schematic, Fig.4-1). The evaporator section and the liquid trap reservoir are coupled by a brass thermal mass. This prevents liquid entrapment from causing premature "dry-out" during the reverse to forward mode transition. It also facilitates the execution and analysis of the diode reverse mode shutdown. The condenser leg has an integral stainless steel saddle for attachment to the HEPP's main radiator. Stainless steel tabs are positioned at six other locations for attachment to the HEPP's structural frame.

The stainless steel liquid trap reservoir is sized to contain the entire fluid inventory. The reservoir's inner wall is circumferentially grooved to promote liquid condensation. A cylindrical slab wick formed from continuous wraps of 30 mesh stainless steel screen is inserted in the reservoir to retain the condensed liquid. Bridges formed from 100 mesh screen are attached to this wick to allow for communication with the threaded reservoir wall. The reservoir is connected with the heat pipe through a stainless steel U-shaped tube. The tube's inner diameter is sufficiently large to prevent capillary interaction between the axial grooves and the liquid trap.

TABLE 2-2
LIQUID TRAP DIODE HEAT PIPE
DESIGN SUMMARY

Wick Configuration

Heat pipe	Axially grooved 20 grooves
Liquid trap reservoir	30 mesh cylindrical slab, 100 mesh bridges, circumferentially grooved wall

Material

Stainless Steel

Working Fluid

Ethane - 9.0g

Operating temperature

180°K

Geometry

	<u>in.</u>	<u>cm</u>
Heat pipe O.D.	.413	1.05
Heat pipe lengths		
Overall	46.85	119.0
Evaporator	4.0	10.16
Adiabatic	24.45	62.10
Condenser	18.40	46.74
Effective	35.65	90.55
Reservoir O.D.	1.00	2.54
Reservoir length	4.00	10.16

Internal pressure @ 70°C

815 psia

Burst safety factor @ 70°C

9.5

The heat pipe is charged with ethane, a fluid which is compatible with the stainless steel envelope and which provides the best fluid properties at the 180°K design temperature.

2.3 Thermal Switch Heat Pipe

The thermal switch is fabricated from two identical lengths of stainless steel axially grooved tubing. These pipes are joined at the evaporators by a U-shaped connecting tube. This joint permits vapor communication but prevents capillary interaction, similar to the diode's liquid trap joint. An aluminum block is clamped to both legs at the evaporator. The heat pipe is charged with methane and designed to operate at 120°K. A design summary of the thermal switch is presented in Table 2-3 (see instrumentation schematic in Fig. 4-5).

The objective of this design is to demonstrate the ability of the heat pipe to protect the heat source during a heat sink temperature excursion. Each leg of the thermal switch has a condenser. The heat pipe transports the heat source energy to whichever leg is colder. Reverse mode heat piping action to the forward mode evaporator will not occur as long as one of the heat sinks is below the heat source temperature.

This thermal control component would be useful in a spacecraft application where radiators experience alternate periods of solar and deep space exposure. The heat source could be coupled via a heat pipe to two or more radiators having different solar profiles. Hence, the heat source would always have a deep space heat sink for energy dissipation. Also, the reverse mode energy input from the solar irradiated side would

TABLE 2-3
THERMAL SWITCH HEAT PIPE
DESIGN SUMMARY

Wick configuration	Axially grooved, 20 grooves	
Material	Stainless steel	
Working fluid	Methane - 2.5 g	
Operating temperature	120°K	
Geometry	<u>in.</u>	<u>cm</u>
Heat pipe O.D.	0.413	
Heat pipe lengths*		
Overall	19.5	49.5
Evaporator	2.0	5.1
Adiabatic	5.5	14.0
Condenser	12.0	30.5
Effective	12.5	31.8
Connecting tube length	5.80	14.7
Centerline to centerline distance	4.0	10.2
Internal pressure @ 40°C	885 psia	
Burst safety factor @ 40°C	7.4	

*Dimensions are given for one of the two identical legs.

be limited to the low axial conduction capacity of the thin walled stainless steel tubing.

2.4 Hybrid Variable Conductance Heat Pipe

This thermal control heat pipe consists of a conventional VCHP design with a liquid trap reservoir attached to the evaporator in the same manner as the diode described in Section 2.2. The gas reservoir provides temperature control for varying sink and power conditions and the liquid trap provides diode performance. A design summary is listed in Table 2-4 and a schematic of the pipe is shown in Fig. 4-8.

The stainless steel cylindrical gas reservoir is interfaced with the grooved tubing via a thin walled stainless steel transition piece that minimizes conduction effects. Liquid communication between the heat pipe and reservoir is accomplished by several layers of 200 mesh stainless steel screen. This transition wick is spotwelded to the heat pipe's grooved wall and to the two layers of 200 mesh stainless steel screen that cover the gas reservoir's interior for liquid distribution purposes.

The reservoir provides a 15.7:1 storage volume ratio. A brass saddle is soldered to the gas reservoir to permit interfacing with the test fixture.

The liquid trap reservoir has the same configuration as the diode's reservoir described in Section 2.2. It is thermally coupled with the evaporator section by an aluminum thermal mass.

The heat pipe is charged with methane, the working fluid, and helium, a non-condensable gas at the 120°K nominal operating temperature.

TABLE 2-4

VARIABLE CONDUCTANCE HEAT PIPE

DESIGN SUMMARY

Wick configuration	Axially grooved, 20 grooves	
Heat pipe	2 layers of 200 mesh spot welded to wall	
Gas reservoir	200 mesh slab	
Transition	30 mesh cylindrical slab, 100 mesh bridges, circumferentially grooved wall	
Liquid trap reservoir	Stainless steel	
Material	Methane - 6.7 g	
Working fluid	Helium - 0.1 g	
Non-condensable gas	120°K	
Operating temperature		
Geometry	<u>in.</u>	<u>cm</u>
Heat pipe O.D.	.413	1.05
Heat pipe lengths		
Overall	30.65	77.9
Evaporator	4.0	10.2
Adiabatic	15.4	39.1
Condenser	11.25	28.6
Effective	23.03	58.5
Gas reservoir O.D.	2.0	5.08
Gas reservoir length	4.45	11.3
Transition O.D.	.313	0.79
Transition length	2.16	5.49
Liquid trap length	3.50	8.9
Liquid trap O.D.	1.0	2.54
Internal pressure @ 40°C	535 psia	
Burst safety factor @ 40°C	7.7	
Gas reservoir/condenser storage ratio	15.7	

3.0 FABRICATION AND PROCESSING

3.1 General

The three thermal components were processed and assembled in accordance with the "Quality Assurance Plan for HEPP Axially Grooved Diode Heat Pipe."² Modifications were made, as required to accommodate the differences among the heat pipe configurations, but the cleaning, inspection, integrity verification, charging, and closure operations were essentially performed as detailed and referenced in the Q/A plan.

3.2 Integrity Verification

The heat pipes are designed to operate in the cryogenic temperature range and, therefore, contain working fluids (methane and ethane) which have high vapor pressures at room temperature. To verify the pressure retention capabilities of these units, each was ammonia leak checked and proof pressure tested. In addition, three tubing samples were burst tested.

The ammonia leak testing did not reveal any porous zones. A proof pressure test was conducted by pressurizing each heat pipe assembly to two times the maximum design operating pressure for ten minutes. The resultant yield measured afterwards was approx. 0.1% in all cases. The three tubing samples that were burst all demonstrated a pressure retention capability well in excess of the four times safety factor required. A summary of the pressure tests is presented in Table 3-1.

TABLE 3-1

PRESSURE RETENTION CHARACTERISTICS OF TCHP's

	<u>Liquid Trap Diode</u>	<u>Thermal Switch</u>	<u>Hybrid VCHP</u>
Maximum operating temperature (°C)	70	40	40
Maximum operating pressure (N/M ²) (psia)	0.562×10^7 (815)	0.610×10^7 (885)	0.369×10^7 (535)
Proof pressure (N/M ²) (psia)	1.103×10^7 (1600)	1.447×10^7 (2100)	0.793×10^7 (1150)
Maximum percent yield in proof pressure test	0.1%	0.1%	0.1%
Burst pressure (N/M ²) (psia)	5.341×10^7 (7750)	4.535×10^7 (6580)	3.722×10^7 (5400)
Tubing safety factor	9.5	7.4	10.1

4.0 THERMAL TESTING

4.1 General

The thermal control heat pipes were tested in a thermal vacuum chamber at B & K Engineering's laboratory. Each heat pipe mounted to a test fixture that provided the interfaces, instrumentation, and thermal control (via heaters and liquid nitrogen cold plate) required in the "Test Procedure for Cryogenic Axially Grooved Heat Pipes."³ Each set-up was covered with multi-layer insulation blankets and mounted to low conductivity supports to minimize parasitics.

4.2 Liquid Trap Diode Heat Pipe

The test results for the diode have already been reported in detail in the "Test Report for HEPP/LDEF Axially Grooved Heat Pipe."⁴ These results are presented again in this section.

The heat pipe configuration and test schematic is presented in Fig. 4-1.

4.2.1 Start-up Test

A 2-W load was applied to the evaporator block as the heat pipe's sink temperature was rapidly decreased from ambient ($\sim 293^{\circ}\text{K}$) to low temperature ($\sim 180^{\circ}\text{K}$). Axial temperature profiles exhibited by the diode during the transition to low temperature isothermal operation are presented in Fig. 4-2. The evaporator's temperature decreased steadily as the diode transported heat from the thermal mass to the cold plate. The heat pipe was isothermal within 110 minutes. Similar behavior was observed during the testing of a prototype unit.⁵

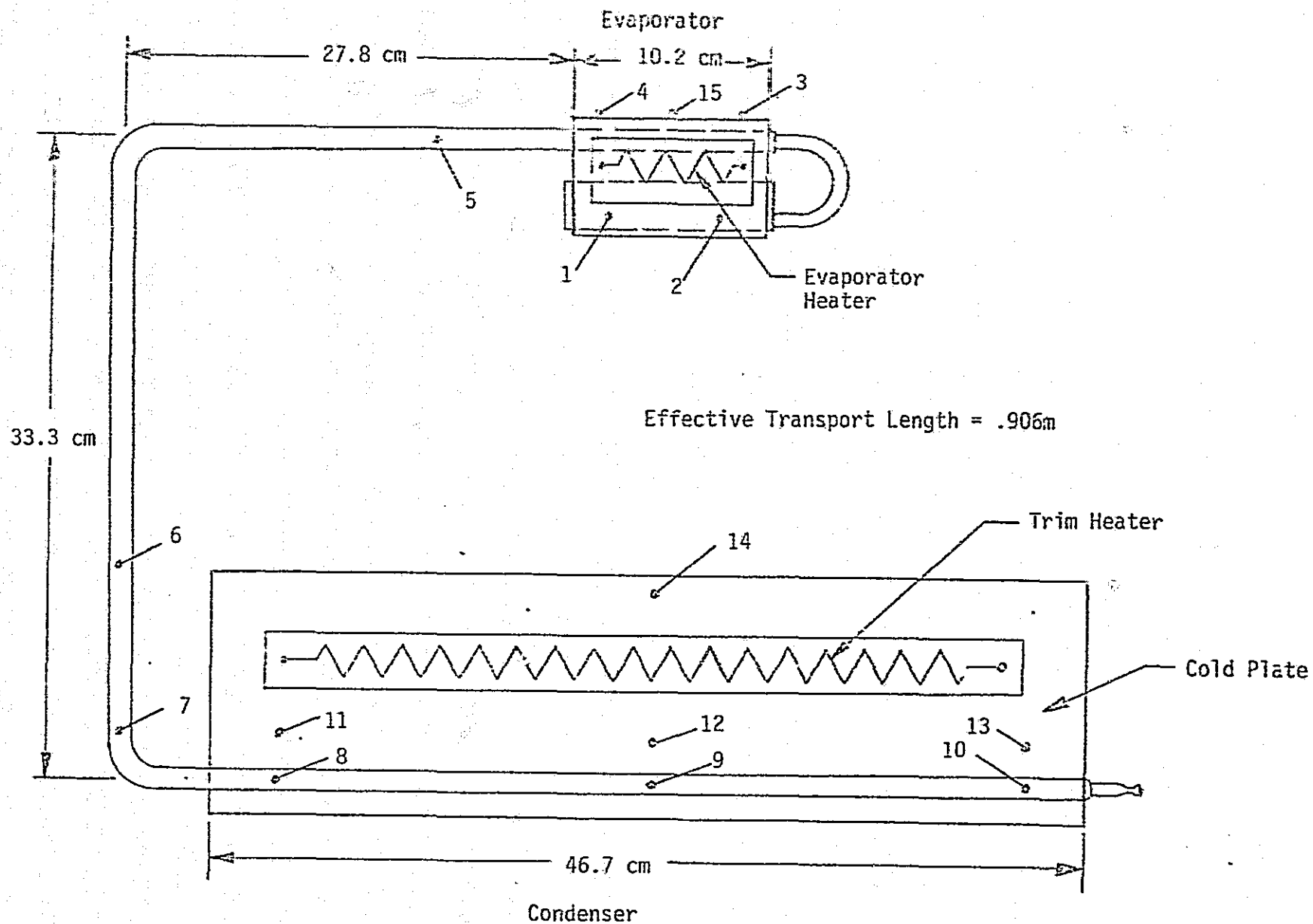


Fig.4-1. HEPP Liquid Trap Diode Heat Pipe Instrumentation Schematic

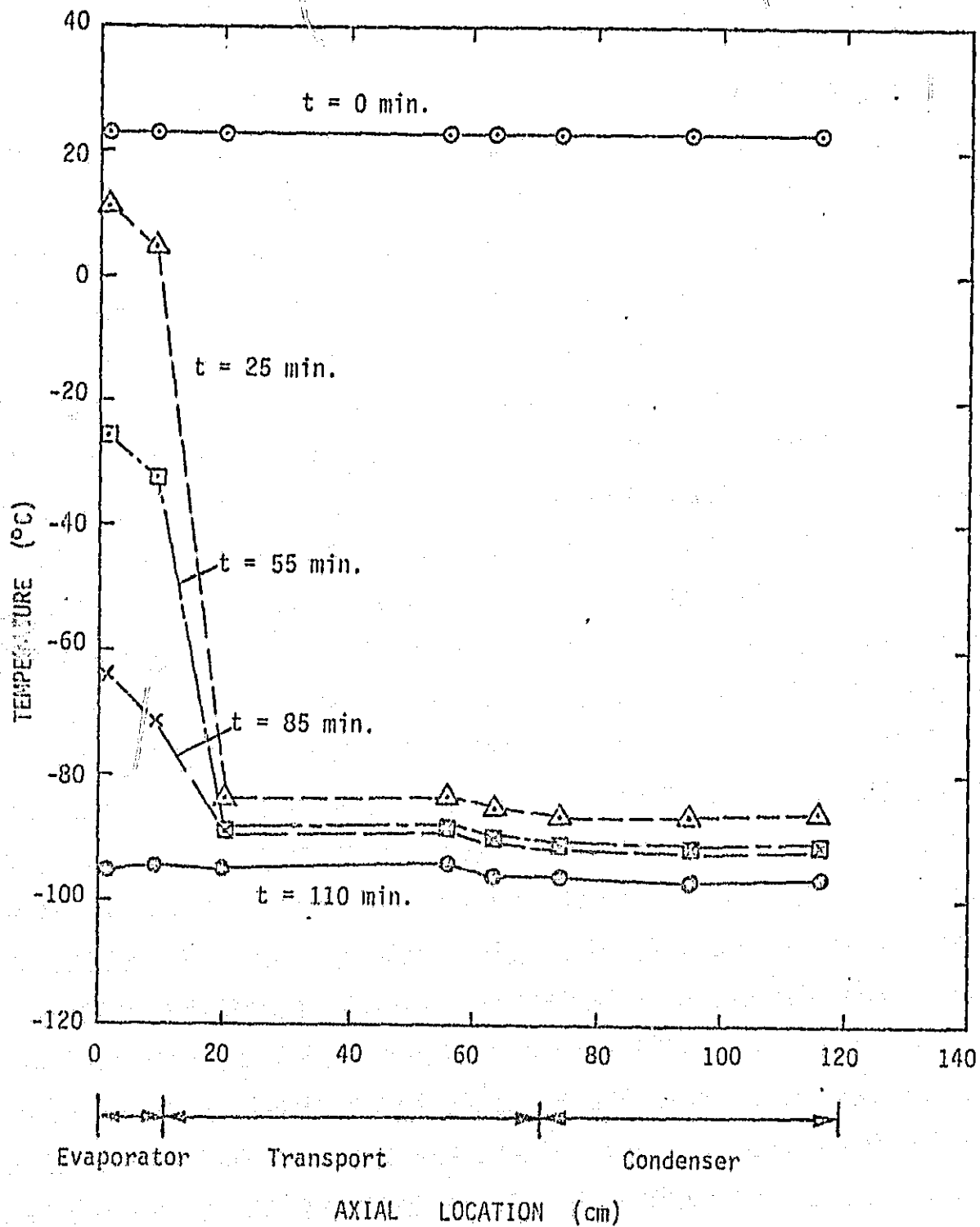


Fig. 4-2. Start-up behavior of liquid trap diode heat pipe under a 2-W load

The transient profile of the evaporator block during the start-up test indicates that the heat pipe was removing energy from the block at an average rate of 11.8-W, in addition to the 2.0-W heater load. For the 0.906-m effective transport length, this corresponds to a heat transport capability of 12.5 W-m at 3.5 mm. The prototype diode heat pipe transported 10.5 W-m at 2.0 mm and 12.3 W-m at 2.4 mm during its start-up tests.

4.2.2 Forward Mode Transport Tests

The LTD was subjected to forward mode transport tests at three elevations (3.6, 5.1, and 6.4 mm) at both the 180°K design temperature and at 150°K. The test results and the predicted performance are presented in Fig. 4-3. The predicted performance of the stainless steel axial groove form was derived from closed-form solutions developed in Ref. 6. A summary of the measured and predicted values for maximum "O-g" heat transport and static height are presented in Table 4-1.

TABLE 4-1 HEPP Liquid Trap Diode Performance

Temperature (°K)	Maximum "O-g" Heat Transport (W-m)		Static Height (mm)	
	<u>Predicted</u>	<u>Measured</u>	<u>Predicted</u>	<u>Measured</u>
150	11.8	9.8	11.7	10.0
180	16.3	18.5	9.7	8.4

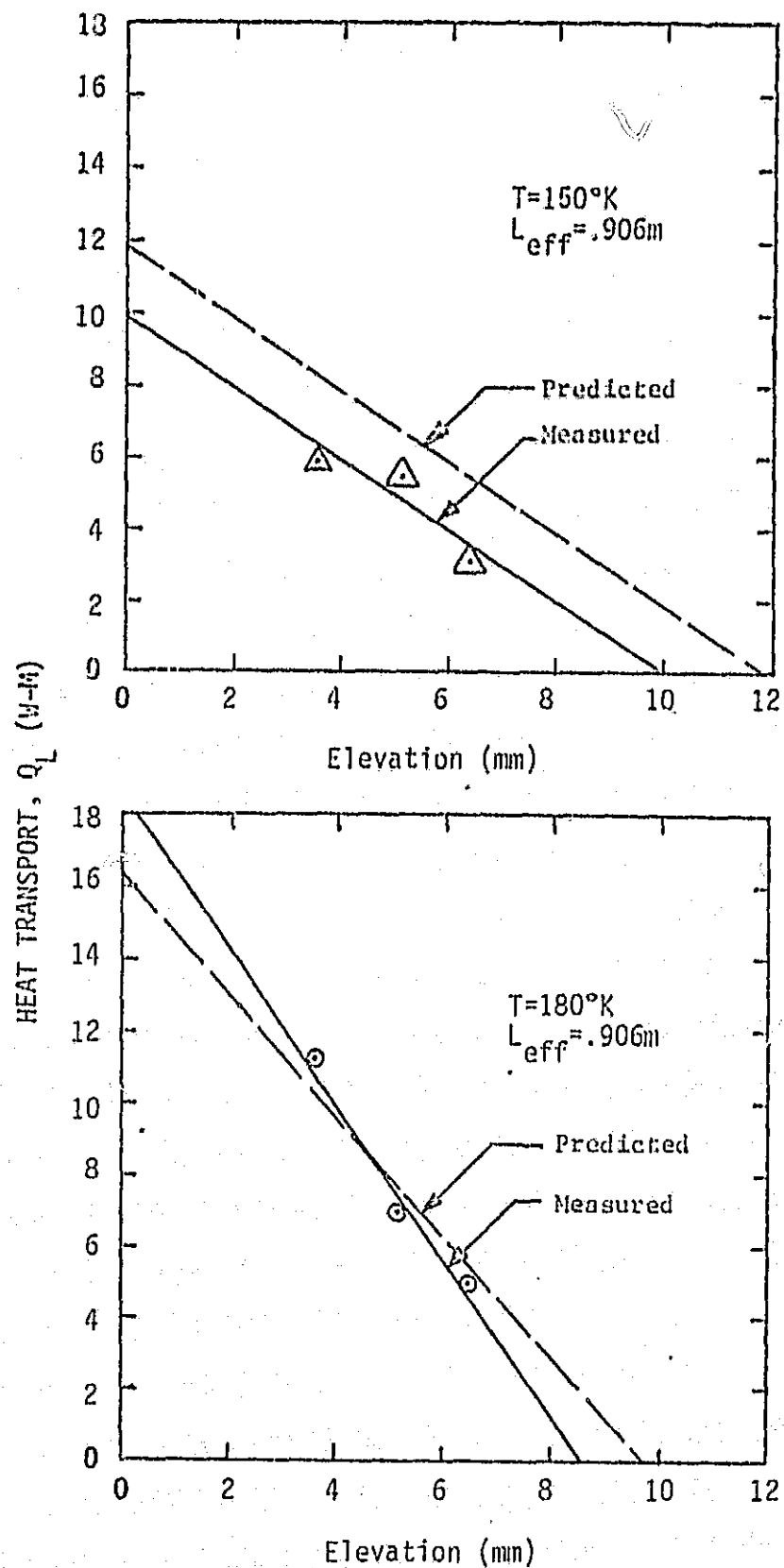


Fig. 4-3. Forward mode heat transport capability of liquid trap diode

The recovery behavior of the liquid trap was observed by decreasing the evaporator heat load by 1 to 2-W following evaporator dry-out. In all tests, the LTD recovered after the load was reduced.

4.2.3 Diode Reverse Mode

This test is initiated with the diode heat pipe in a steady-state forward mode condition. The power on the trim heater is increased, thereby raising the sink temperature above the evaporator temperature and initiating reverse mode operation.

The temperature profile exhibited during reverse mode testing is presented in Fig. 4-4. The test was initiated at $t = 1$ min. At this time the heat pipe was operating at approximately 180°K under a 1-W evaporator heat load. At $t = 8$ min the condenser section had completely dried out. The evaporator block absorbed 1.11 W-hr of energy, exclusive of parasitics, during the condenser shutdown. This corresponds to 89% of the latent energy associated with the ethane fluid inventory. By $t = 24$ min, the transport section had shutdown to within 10 cm of the evaporator section. The evaporator block absorbed a total of 1.64 W-hr during this 23 min. shutdown period; i.e., 132% of the latent energy of the fluid charge. However, the additional 0.53 W-hr absorbed by the evaporator block during the shutdown of the transport section is largely due to parasitic input rather than axial conduction.

The prototype unit of the liquid trap diode exhibited similar reverse mode behavior. During condenser shutdown its thermal mass absorbed the equivalent of 85% of the fluid inventory's latent energy.

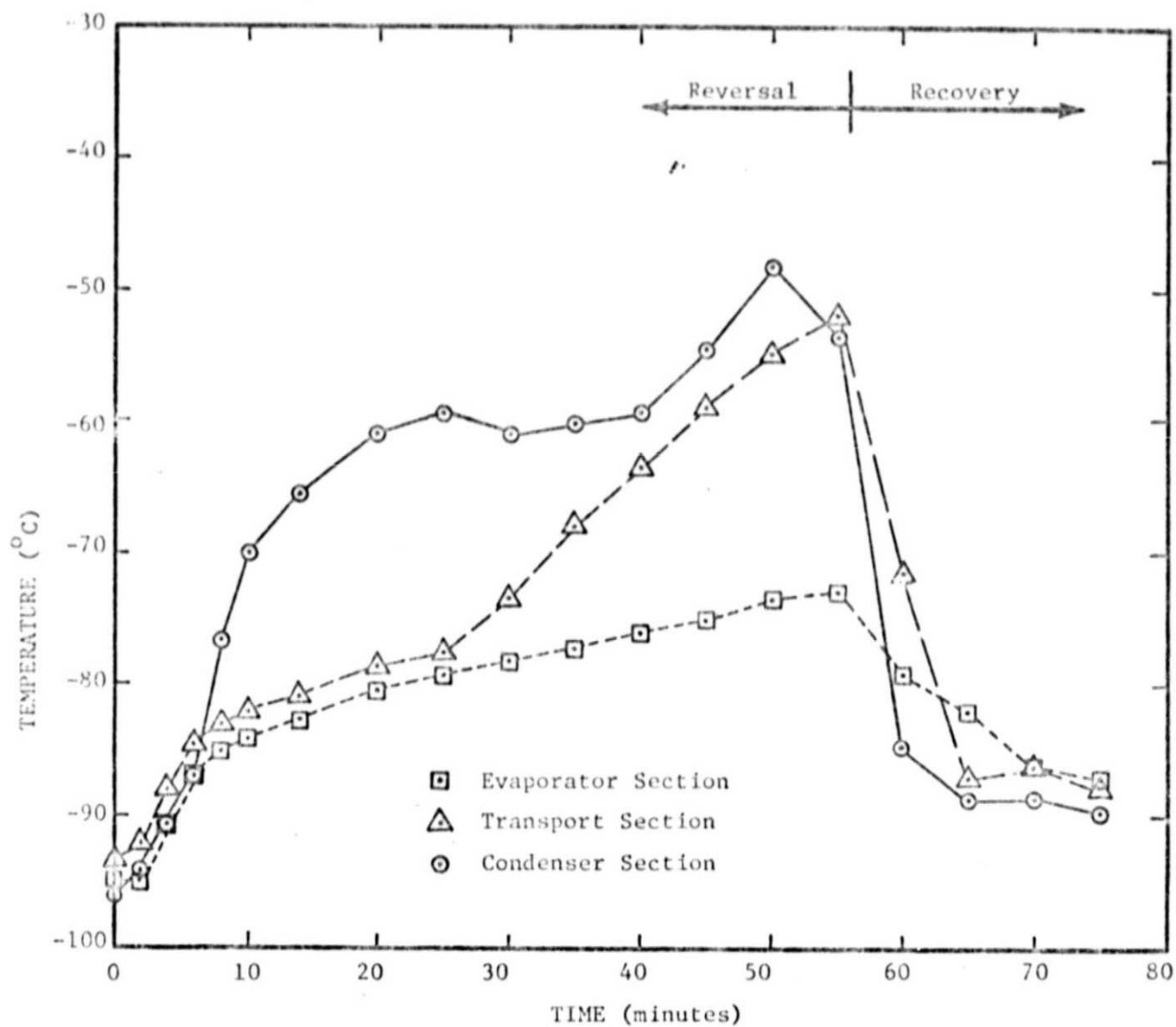


Fig. 4-4. Reversal and recovery behavior of the liquid trap diode heat pipe.

Following shut-down, a recovery test was initiated at $t = 56$ min. by allowing the sink temperature to drop below the evaporator temperature to 180°K (see Fig. 4-4). Also, a 5-W load was applied to the evaporator at $t = 61$ min. By $t = 70$ min., or 14 min. after complete shutdown, steady-state forward mode operation was again achieved. Similar behavior was observed during prototype testing.

4.3 Thermal Switch Heat Pipe

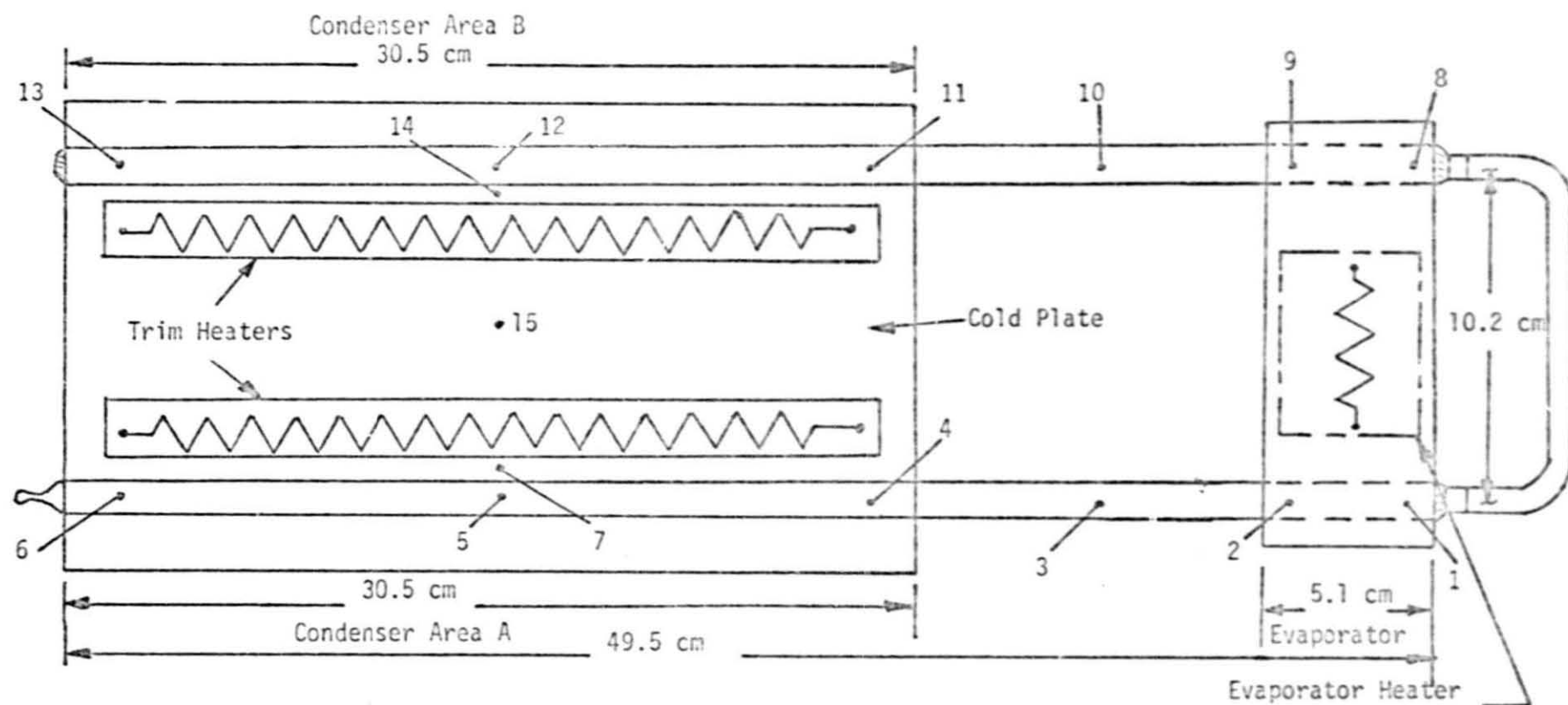
The thermal switch with its associated test instrumentation is presented in Fig. 4-5.

4.3.1 Forward Mode Transport Test

Each leg of the switch was tested at three elevations to determine its transport capability. While one leg was being tested at approximately 120°K , the other condenser section was maintained at 160°K to prevent condensation and keep that leg dried out. The transport capability measured in these tests is plotted in Fig. 4-6 along with the predicted performance. The maximum 0-g transport capacity derived from testing was 9.4 W-m; the predicted value was 12.9 W-m. The heat pipe recovered when the load was reduced by 2-W.

4.3.2 Switching Operation

The purpose of this test was to demonstrate the ability of this system to shut down forward mode operation in one leg and switch to the other. This was accomplished by interchanging the sink conditions of the two legs via the trim heaters while a constant 2-W load was applied to the evaporator. The condenser section initially maintained at 120°K was raised



Effective Transport Length = 0.318 m

Fig. 4-5 Thermal Switch Heat Pipe Instrumentation Schematic

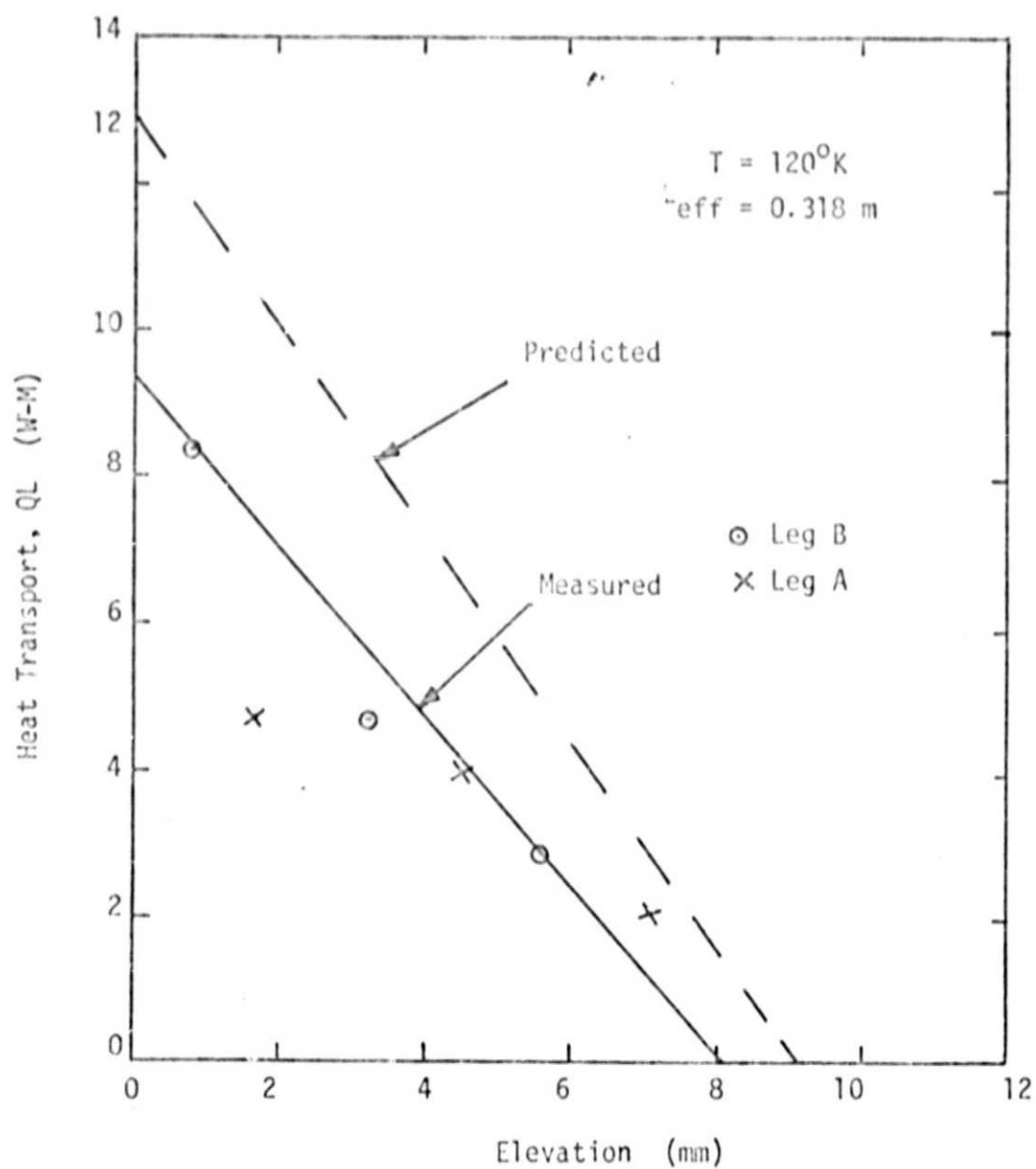


Fig. 4-6 Heat transport capability vs. elevation
for thermal switch heat pipe

to 160°K while the other leg was simultaneously lowered from 160°K to 120°K.

A typical switching operation is plotted in Fig 4-7. At $t = 0$ minutes, leg A is transporting 2-W and leg B is shutdown. Immediately afterwards the inputs to the two trim heaters are switched. This initiates a reversal of the sink conditions. Between $t = 0$ min. and $t = 2$ min., both condenser legs are higher in temperature than the evaporator. Therefore, the 2-W input to the evaporation block is not transported away and the block rises almost 4°C in temperature. As the temperature of heat sink B drops below the evaporator, heat pipe action starts again and the evaporator temperature begins to drop (between $t = 2$ min. and $t = 4$ min.). Within seven minutes, the profiles have reversed and the evaporator block is back to its original temperature.

4.4 Hybrid VCHP

The VCHP was fabricated and tested in the hybrid configuration; i.e., with the liquid trap reservoir communicating with the VCHP. A test schematic is presented in Fig. 4-8.

4.4.1 Start-Up

The temperature profiles exhibited by the Hybrid VCHP as it cooled from ambient temperature ($\sim 300^\circ\text{K}$) to its design operating temperature ($\sim 120^\circ\text{K}$) are presented in Fig. 4-9. Within 30 min. the vapor temperature of the pipe

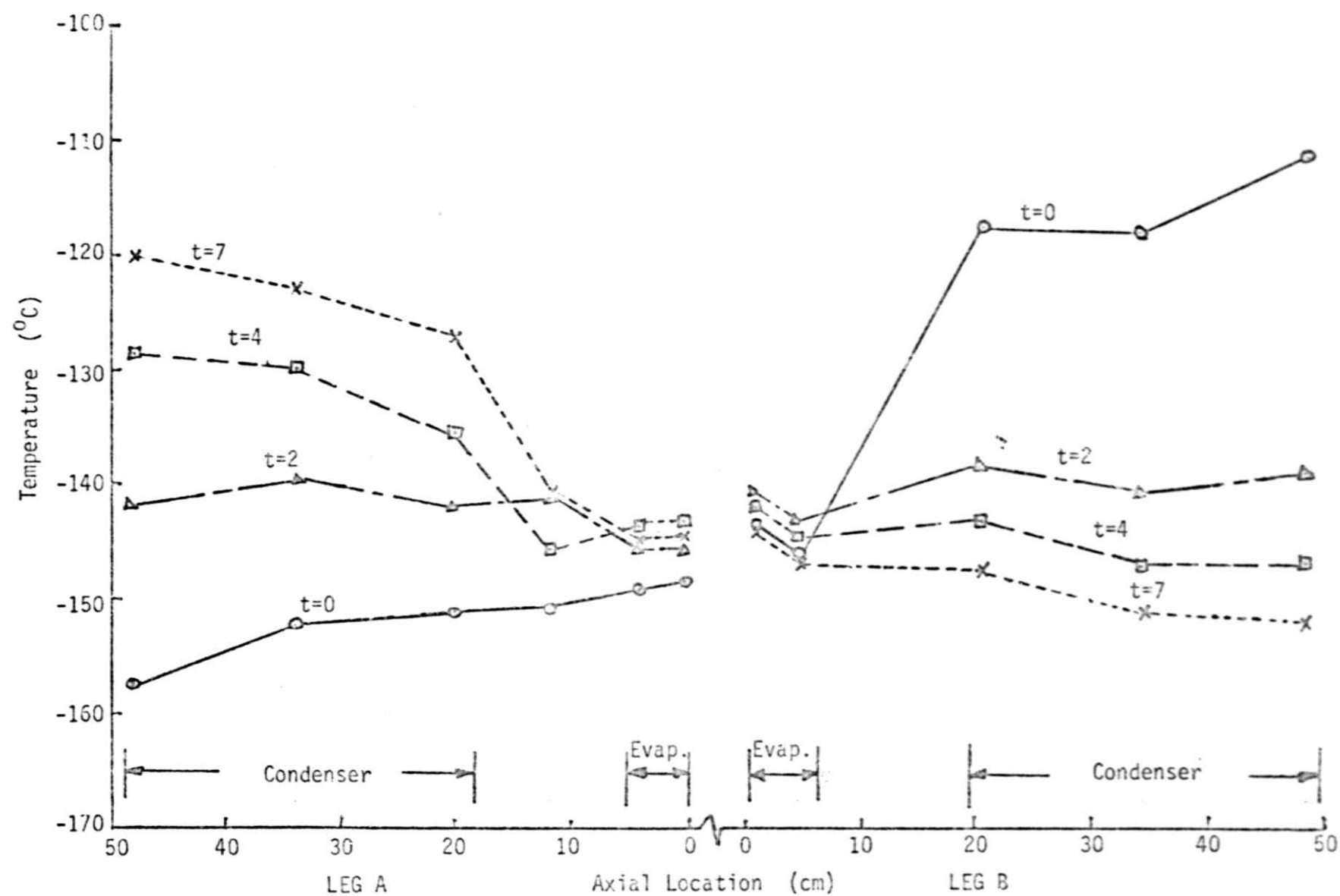


Fig.4-7 Axial profiles of thermal switch heat pipe during switching operation

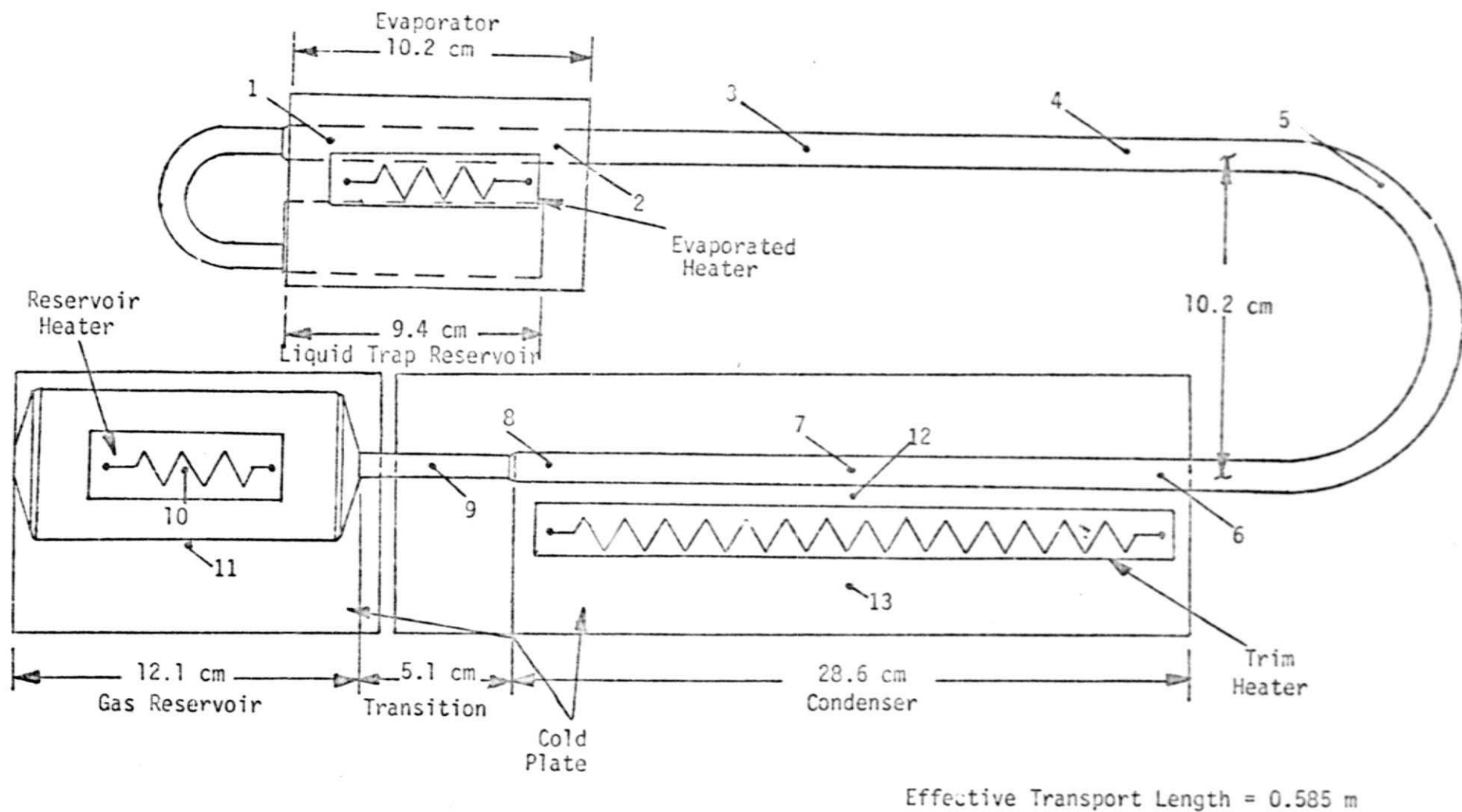


Fig.4-8 Hybrid VCHP Instrumentation Schematic

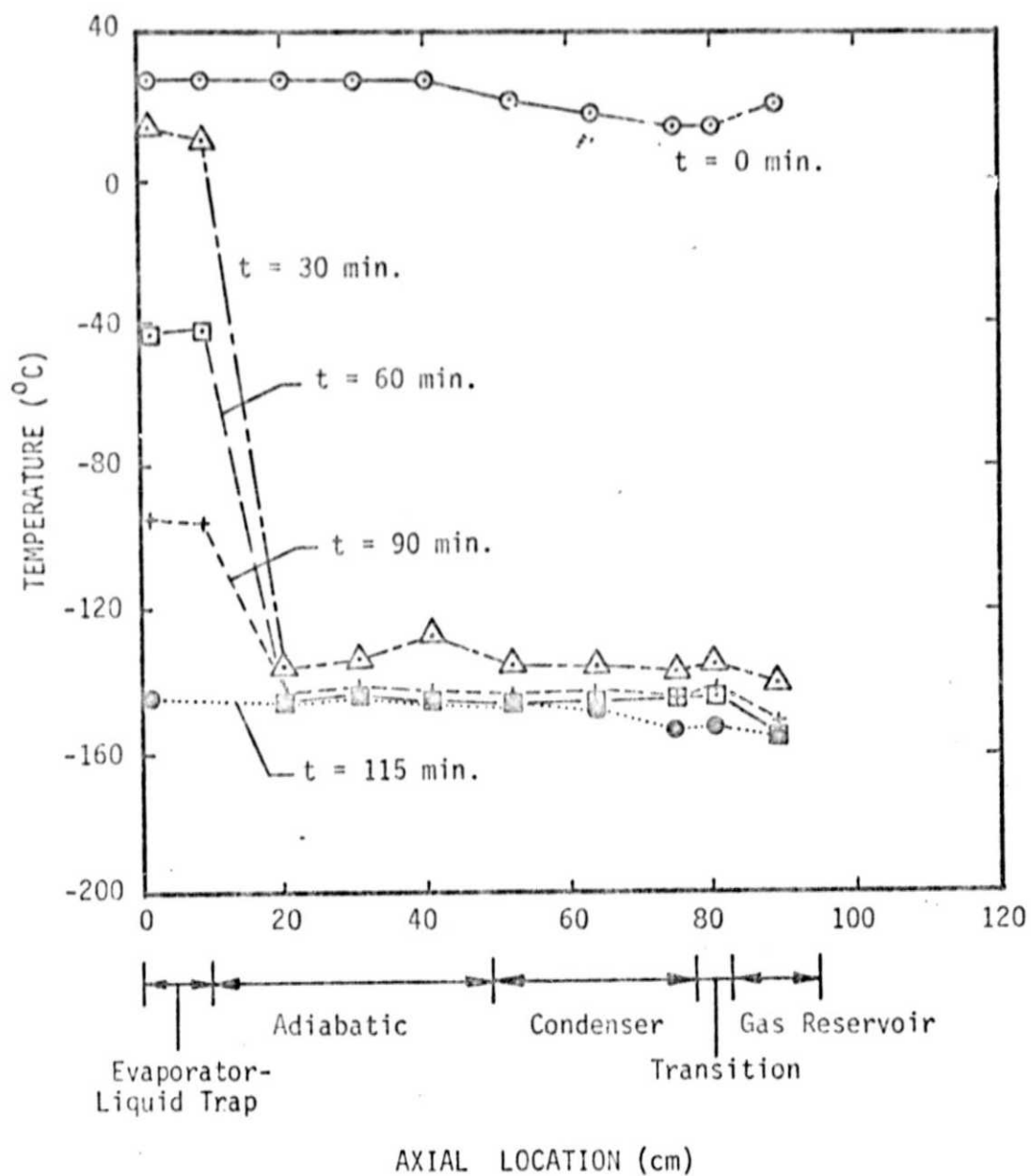


Fig.4-9 Start-up behavior of VCHP/hybrid

is low enough to permit heat piping and the temperature of the evaporator thermal mass begins to decrease. Within 115 min., the pipe is isothermal. The heat transport (exclusive of parasitics) derived from the thermal mass behavior in two start-up tests was 8.1 W-m and 7.8 W-m.

4.4.2 Forward Mode Transport

The forward mode transport tests were conducted at three (3) elevations with an operating temperature of approximately 125°K. The test results and the predicted values are shown in Fig. 4-10. The maximum 0-g heat transport and static height derived from the tests were 9.2 W-m and 8.4 mm, respectively. The predicted values, determined by a closed-form solution based on groove geometry and fluid properties, were a 19.0 W-m transport capacity and a 9.7 mm static height. The heat pipe consistently recovered after evaporator dry-out when the power was reduced slightly (1 to 3-W).

There are several possible explanations for the disparity between the measured and predicted transport capacities. One is that unaccounted-for parasitic inputs effectively reduce transport performance as measured by evaporator heat input. This effect can be significant in the cryogenic region. Another explanation would be an effective undercharge of working fluid. This could be caused by fluid entrapment in one of the reservoirs as well as by actual under charge.

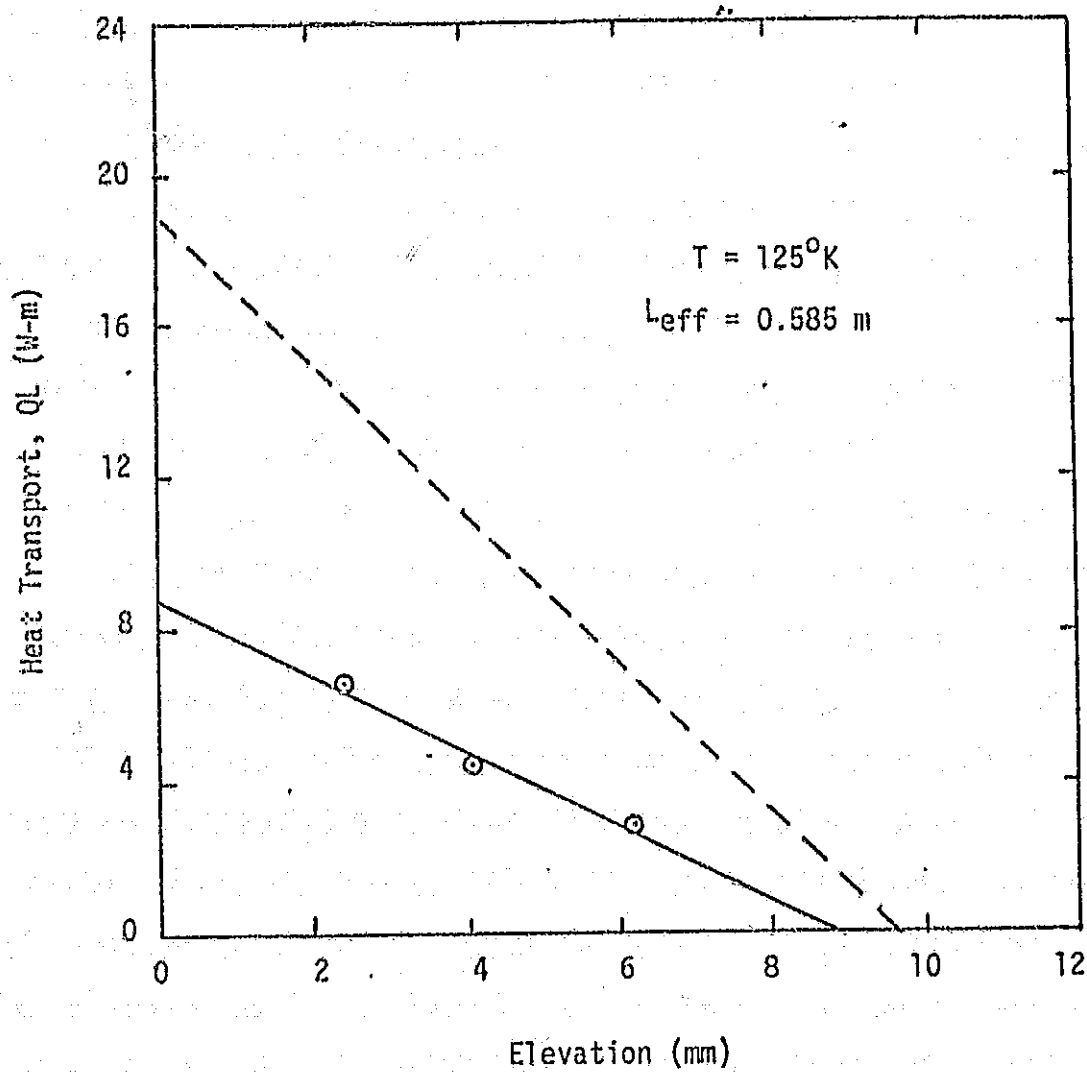


Fig. 4-10 Heat transport capability vs. elevation for Hybrid VCHP

Finally, it has been noted that degraded forward mode performance frequently occurs in VCHPs.^{7,9} It appears that condensation is concentrated behind the advancing gas/vapor front rather than being spread uniformly over the condenser length. This could result in a condensation film layer that is thick enough to induce drainage of the upper grooves. Also, if the front is located between the condenser midpoint and the gas reservoir (as it was in these tests) the effective transport length is increased and the heat load capacity proportionately decreased.

4.4.3 Variable Conductance Behavior

The VCHP was tested at a high power-high sink and a low power-low sink condition to determine the thermal control provided by the gas reservoir. The low power-low sink condition was evaluated with both passive and constant temperature gas reservoir control. A summary of the test results is presented in Table 4-2.

The vapor temperature dropped 13.9°C going from the high to low condition with passive control and only 3.1°C with constant temperature reservoir control. An analysis based on the VCHP's configuration and the test's boundary conditions yields theoretical vapor temperature drops of 19.0°C and 1.8°C for the passive and constant temperature modes respectively.

4.4.4 Diode Reverse Mode

The diode reverse mode test for the Hybrid VCHP is conducted in the same manner as the liquid trap diode reversal. Initially the heat pipe was operating in the forward mode under steady state conditions. The evaporator power is then removed and the power of the heaters attached to the reservoir

Table 4-2

SUMMARY OF HYBRID VCHP GAS CONTROL TESTS

	<u>High Power-High Sink</u>	<u>Low Power-Low Sink</u>	
		<u>Passive</u>	<u>Constant Temp. Reservoir</u>
Vapor Temperature ($^{\circ}\text{K}$)	125.4	111.5	122.3
$\Delta T_{V_{h-1}}$ ($^{\circ}\text{K}$)		13.9	3.1
Sink Temperature ($^{\circ}\text{K}$)	122.8	87.0	92.2
$\Delta T_{O_{h-1}}$ ($^{\circ}\text{K}$)		35.8	30.6
Reservoir Temperature ($^{\circ}\text{K}$)	115.6	87.1	114.5
$\Delta T_{r_{h-1}}$ ($^{\circ}\text{K}$)		28.5	1.1
Evaporator Power (W)	10.0	0.0	0.0
Trim Heater Power	ON	OFF	OFF
Reservoir Power	ON	OFF	ON

and condenser sinks increased (at $t = 16$ min. in Fig. 4-11). The temperature profiles exhibited by the hybrid VCHP are shown in Fig. 4-11.

Within 10 minutes ($t = 26$ min.) the entire condenser section was dried-out. At this time the gas reservoir temperature caught up with the evaporator. It followed the evaporator profile briefly as the methane charge, retained by the reservoir wick, was transported to the evaporator. By $t = 30$ min. all the fluid had evaporated as indicated by the increased rate of temperature rise of the gas reservoir.

When the fluid in gas reservoir evaporated and flowed to the liquid trap, it carried with it the noncondensable gas charge. This may explain why the adiabatic section did not dry-out eventually, as it did with the liquid trap diode. It continued to transport parasitics to the evaporator thermal mass.

The VCHP was effectively shutdown within 14 minutes. During this interval, the evaporator thermal mass absorbed 0.89 W-hr of energy, exclusive of parasitics. This corresponds to 102% of the latent energy of the methane fluid inventory.

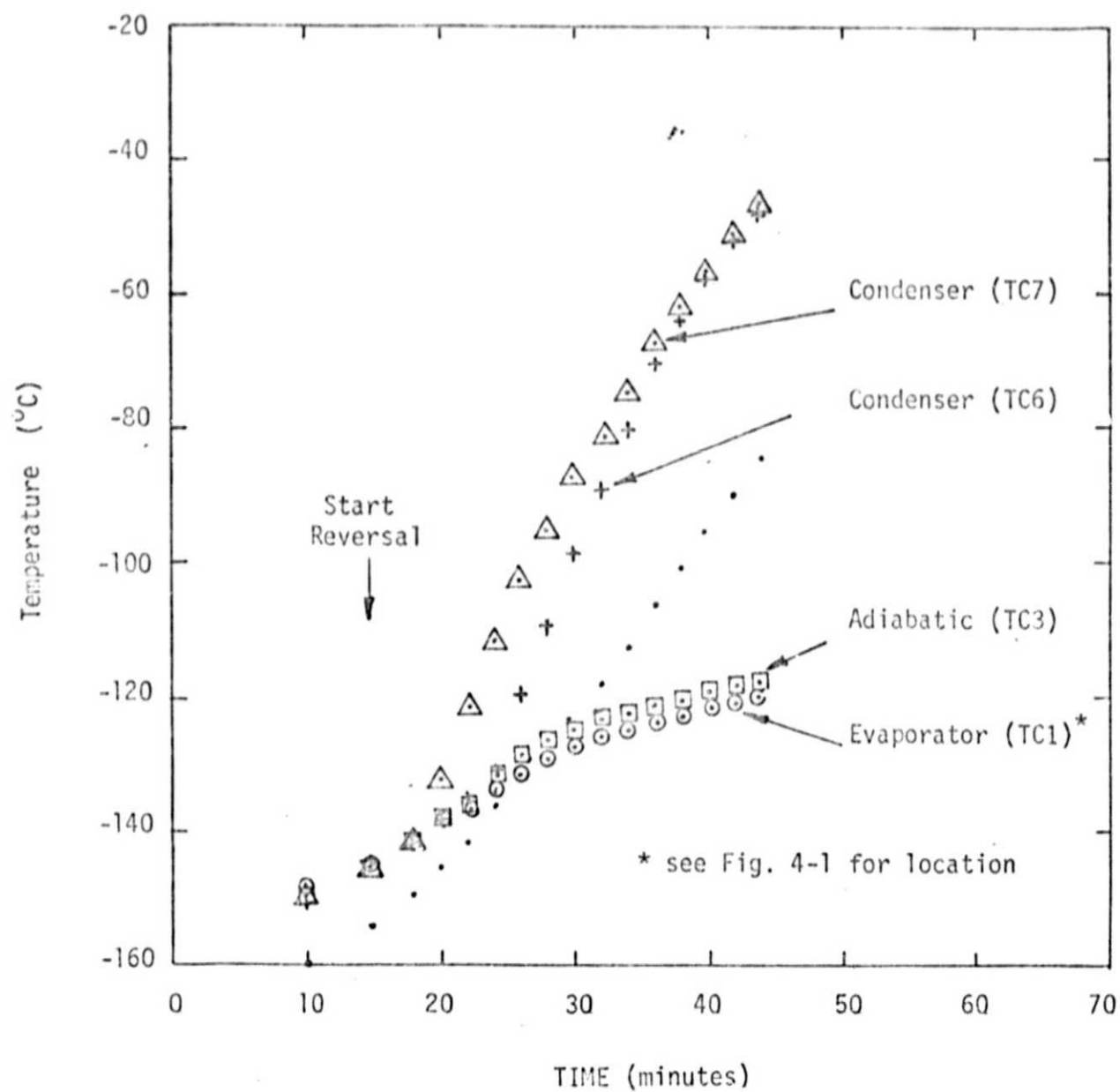


Fig. 4-11 Hybrid VCHP diode reversal behavior.

5.0 CONCLUSIONS AND SUMMARY

This program has demonstrated that axially grooved heat pipes fabricated from stainless steel can be successfully employed as thermal control components in the low temperature to cryogenic range. Three heat pipes, including a liquid trap diode, a thermal switch and a hybrid VCHP, were fabricated and tested.

The liquid trap diode heat pipe is designed to be compatible with the requirements of the Heat Pipe Experiment Package (HEPP), which is scheduled for flight aboard the Long Duration Flight Exposure Facility (LDEF). This heat pipe exhibited a maximum 0-g heat transport capacity of 18.5 W-m and a static wicking height of 8.4 mm at the 180°K design operating temperature. During a typical diode reverse mode test, the condenser section was completely dried out within seven minutes. The evaporator thermal mass absorbed 1.11 W-hr of energy, exclusive of parasitics, during condenser shutdown. This corresponds to 89% of the latent energy associated with the ethane charge.

The thermal switch heat pipe demonstrated a maximum 0-g heat transport of 9.4 W-m and a static wicking height of 8.1 mm at the 120°K design temperature. While the heat piping condenser leg was operating at 120°K, the other leg was maintained at 160°K, keeping it effectively shutdown. When the sink conditions were reversed, the heat pipe switched legs almost immediately.

The hybrid VCHP is designed to perform as a conventional VCHP and also as a liquid trap diode at a 120°K operating temperature. The maximum 0-g heat transport derived from the forward mode tests was 9.2 W-m and the static wicking height was 8.4 mm. This is 50% of the predicted transport capacity. Degraded performance had been previously observed with other VCHP's. One explanation is that the condensation zone is concentrated directly behind the advancing gas/vapor front. This would increase the effective transport length in the high power-high sink condition. It may also create a condensation film layer that is thick enough to induce drainage of the upper grooves.

The VCHP was tested at high power-high sink and a low power-low sink condition to determine the control provided by the gas reservoir. Both passive and constant temperature reservoir configurations were tested. With a passive reservoir, the vapor temperature dropped 14°C when the sink temperature was lowered by 36°C and the power was reduced from 10-W to 0. When the reservoir was maintained at a constant temperature, the vapor temperature varied only 3°C with a 31°C sink temperature change and a 10-W load reduction. These results compare favorably with predicted values based on the system design and bounding conditions. In terms of controllability, the current VCHP theory is applicable to axially grooved systems in the cryogenic range.

The hybrid VCHP also demonstrated effective diode performance. During a reverse mode test the condenser and the gas reservoir were both dried out within 14 minutes. The evaporator block absorbed 0.89 W-hr of energy (102% of latent heat of methane charge), exclusive of parasitics, during shutdown.

All three heat pipes were capable of start-up when the condenser heat sinks were rapidly lowered from ambient temperature to the design operating temperatures (120°K or 180°K). Each unit recovered completely during the transport tests when the heat load which induced evaporator dry-out was reduced slightly.

The stainless steel axially grooved design appears well suited to cryogenic thermal control applications. The stainless steel tubing provides a high strength envelope which minimizes axial conduction effects. The axially grooved wick configuration provides reliable and repeatable performance during start-up, transport and recovery. Methane and ethane are both compatible with the stainless steel envelope and appear to have well defined properties at their respective 120°K and 180°K design temperatures.

The liquid trap/axially grooved tubing combination provided effective diode performance. The energy absorbed by the evaporator's thermal mass during shutdown was approximately equal to the latent energy of the working fluid. The liquid trap diode consistently recovered during the transition from reverse to forward mode.

6.0 REFERENCES

1. Summary Report for Development of a Cryogenic Axially Grooved Stainless Steel Heat Pipe," BK026-1006, prepared by B & K Engineering, Inc. for NASA/Ames Research Center, September 1977.
2. "Quality Assurance Plan for HEPP Axially Grooved Diode Heat Pipe," BK042-1007, prepared by B & K Engineering, Inc. for NASA/Ames Research Center, March 1978.
3. "Test Procedure for Cryogenic Axially Grooved Thermal Control Heat Pipes," BK042-1001, prepared by B & K Engineering, Inc. for NASA/Ames Research Center, October 1977.
4. "Test Report for HEPP/LDEF Axially Grooved Heat Pipe," BK042-1011, prepared by B & K Engineering, Inc. for NASA/Ames Research Center, June 1978.
5. "Development of Cryogenic Thermal Control Heat Pipes," BK042-1010, B & K Engineering Interim Report, prepared for NASA/Ames Research Center, May 1978.
6. "Summary Report for Axially Grooved Heat Pipe Study," BK012-1009, prepared for NASA/Goddard Space Flight Center by B & K Engineering, Inc., July 1977.
7. Telecon with Roy McIntosh, NASA Goddard Space Flight Center, August 1978.
8. Unpublished B & K Engineering, Inc. data.